ORIGINAL PAPER

Does the spatial pattern of urban blue–green space at city-level affects its cooling efficiency? Evidence from Yangtze River Economic Belt, China

Ren Yujie[1] · Xiaolan Tang[1,2] · Tianhui Fan[3] · Daxi Kang[4]

Abstract

Utilization of urban blue-green spaces had been recognized as an environmentally friendly and politically acceptable approach to mitigate global warming. However, the evidence and hence knowledge of how the spatial pattern of urban blue–green space at city-level affects its cooling efficiency are limited. Therefore, in this paper, we are devoted to clarifying the cooling mechanism of urban blue–green space from the perspective of composition and distribution pattern. To do that, the Yangtze River Economic Belt, which had experienced significant environmental deterioration and contained rich blue–green resources, was taken as the case study site. Besides, the panel regression models and a new quadratic-curve-fitting based threshold effect estimating model were constructed to investigate the impact of spatial pattern of blue–green space on its holistic cooling intensity at city-level and to estimate the optimal spatial layout of blue–green spaces with maximum cooling efficiency. The results evidenced that the proportion and distribution characteristics of forests and shrublands in urban areas improved the intensity of urban cold island effect significantly, while that of grassland and water bodies mitigated urban heat island effect. Moreover, it was demonstrated that the city-level spatial pattern of urban blue–green space has a greater influence on its cooling efficiency at specific time periods (summer and daytime) and regions (mountainous cities with a small population). In addition, it was estimated that the cooling effect reaches the local maximum (around 1.2 ℃) when the PLAND / LSI index of forests, shrublands, grasslands, and water bodies at city-level is about 20%, 0.1%, 42.5% and 15.4% / 38.25, 5.08, 48.25 and 8.54, respectively. We believe our findings contribute significantly to the understanding on the link between ecological land elements and sustainable development of urban ecosystem.

Keywords Ecological land · Cold island · Threshold effect · Urban ecosystem

Introduction

In recent years, with the rapid development of the global economy, the level of infrastructure construction in urban areas has increased significantly. Since urban building complexes, asphalt and concrete roads have greater heat absorption rates and smaller specific heat capacities than suburban soils and vegetation, this has led to generally higher temperatures in urban areas than in the surrounding suburbs. Researchers have summarized this phenomenon as the urban heat island (UHI) effect, which is one of the most significant features of urban climate (Peter 1994; Schneider 1989). The climate phenomena of UHI caused by rapid urbanization had even led to the increase of energy consumption, greenhouse gas emission, and air pollution (Li et al. 2019; Chen and You 2019; Stone 2005). In order to solve these climate deterioration problems compromising human health, the development of urban landscape structures, represented by urban blue–green spaces, has been recognized as an environmentally friendly, and politically acceptable approach to mitigate the UHI effect (Byrne and Yang 2009; Carvalho et al. 2017; Antoszewski et al. 2020;

✉ Xiaolan Tang
  xiaolant@njfu.com.cn

[1] College of Landscape Architecture, Nanjing Forestry University, Nanjing, China

[2] NJFU Academy of Chinese Ecological Progress and Forestry Studies, Nanjing Forestry University, Nanjing, China

[3] International Institute for Carbon-Neutral Energy Research, Kyushu University, Fukuoka, Japan

[4] College of Land Resource and Tourism, Luoyang Normal University, Luoyang, China

Georgiou et al. 2021; Pielke and Avissar 1990). Therefore, how to regulate and locate the landscape structures in urban regions represented by blue–green spaces to cope with urban heat island and other climate phenomena is the focus of current social concern.

Previous studies have revealed that urban blue–green spaces of water bodies, parks, forests, and grasslands showed a strong effect in cooling the land surface temperature (Murakawa et al. 1991; Du et al. 2016; Yan and Dong 2015; Giridharan et al. 2008). While mitigating the UHI effect, they even lead to the appearance of urban cold island (UCI) (Półrolniczak 2017). The size, shape, and connectivity of urban blue–green spaces are demonstrated to be the main factors influencing the cooling effect (Estoque et al. 2017; Gunawardena et al. 2017; Tan et al. 2021). Moreover, researchers also realized that the cooling effect might change significantly when the area of certain types of blue–green space patches exceed a certain value (Yu et al. 2017). It had also been emphasized that the change-point (TVoE) is significant to obtain the maximum cooling efficiency (Yu et al. 2020).

However, studies related to the cooling effect of blue–green spaces mainly shed light on the potential association between single or certain types of blue–green space patches and the land surface temperature but ignored the influence of the global spatial combination and pattern of different categories of blue–green spaces at city scale (Yu et al. 2020). Besides, the heterogeneity of blue–green spaces' cooling effect, especially their influence on UCI effect, in various periods and regions only had been conducted in a few empirical analyses, and the mechanism difference behind was rarely clarified, either.

Therefore, considering the great importance to understand the mechanism of the city-level spatial layout of the landscape infrastructure, represented by urban blue–green space, on its cooling efficiency in response to global warming and the gap within the related fields, we summarized two research questions that still remained to be answered. (1) How does the spatial pattern (composition, distribution and shape) of different categories of blue–green space at city scale affect the intensity of urban cold island effect? (2) What is the optimal spatial pattern of blue–green spaces of the maximum cooling efficiency at city scale? To address these questions, the panel regression models and a new Quadratic-Curve-Fitting based threshold effect estimating model will be constructed in this study to investigate the impact of spatial pattern of blue–green space on its holistic cooling intensity at city-level and to estimate the optimal spatial layout of blue–green spaces with maximum cooling efficiency. From the perspective of academic contribution, this study not only quantifies the impact mechanism of the composition and distribution pattern of blue–green spaces within cities on their cooling efficiency from the meso-urban scale, but also provides a new method and quantitative basis for estimating the layout of blue–green spaces under the scenario of maximizing cooling efficiency. This enhances the understanding on the link between ecological land elements and sustainable development of urban ecosystem.

Methodology

Research procedure

To answer the two research questions proposed in the introduction section, the specific design of this study is as follows (Fig. 1).

Specifically, (1) firstly, through the literature review and the understanding of the trend of the times, we set clarifying the cooling mechanisms of the blue–green spaces from the perspective of composition and distribution and estimating the optimal spatial pattern of blue–green spaces of the maximum cooling efficiency at city-level as the two main objectives of this study. (2) Secondly, the Yangtze River Economic Belt, which had experienced significant environmental deterioration and contained rich blue–green resources, was taken as the case study site. Also, we collected the data related to land cover of blue–green spaces and surface temperature from MCD12Q1, MODIS TERRA and AQUA datasets, respectively, and selected the landscape metrics and SUE algorithm to quantify the spatial pattern of blue–green space as well as the heat / cold island intensity for all cities in the Yangtze River Economic Zone from 2003 to 2018. (3) Thirdly, the panel regression models and a new Quadratic-Curve-Fitting-based threshold effect estimating model were constructed to investigate the impact of spatial pattern of blue–green space on its holistic cooling intensity at city-level and to estimate the optimal spatial layout of blue–green spaces with maximum cooling efficiency. (4) Fourthly, we interpreted the regression results and verified the validity of the threshold estimation model in calculating the optimal blue–green spatial pattern based on the regression and fitting results. (5) Finally, based on the results of the research and discussion, we also put forward targeted views on the construction of blue–green space at the urban scale and related policy recommendations.

Study area

The study area of this work is the Yangtze River Economic Belt (Fig. 2), which had experienced numerous economic and development reforms (Jin et al. 2018). The rapid urbanization of cities in this region has been proved to be one of the most significant driving factors of urban heat island effect and climate warming (Huang and Lu 2015). On the other hand, Yangtze River Economic Belt is rich in various
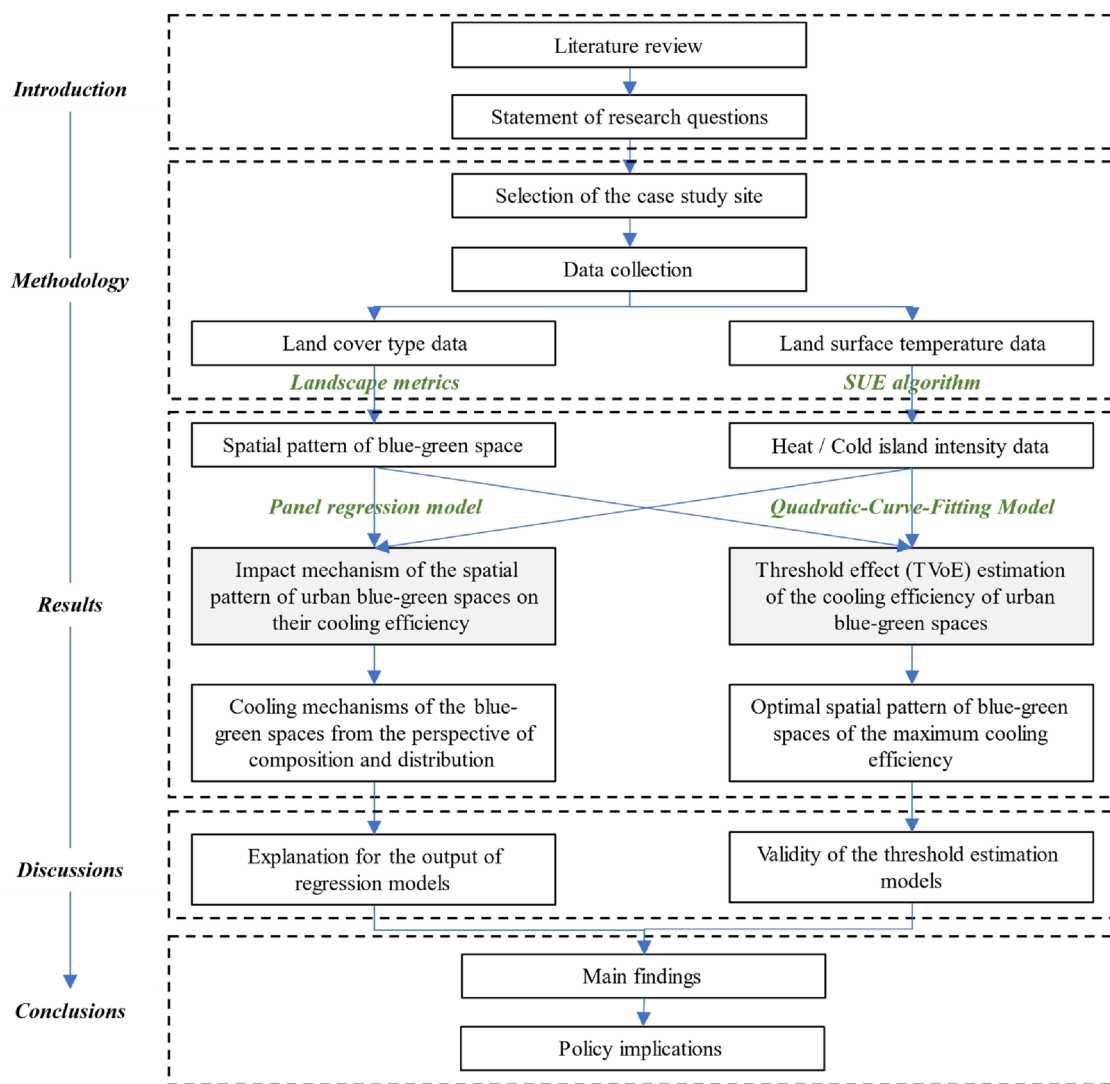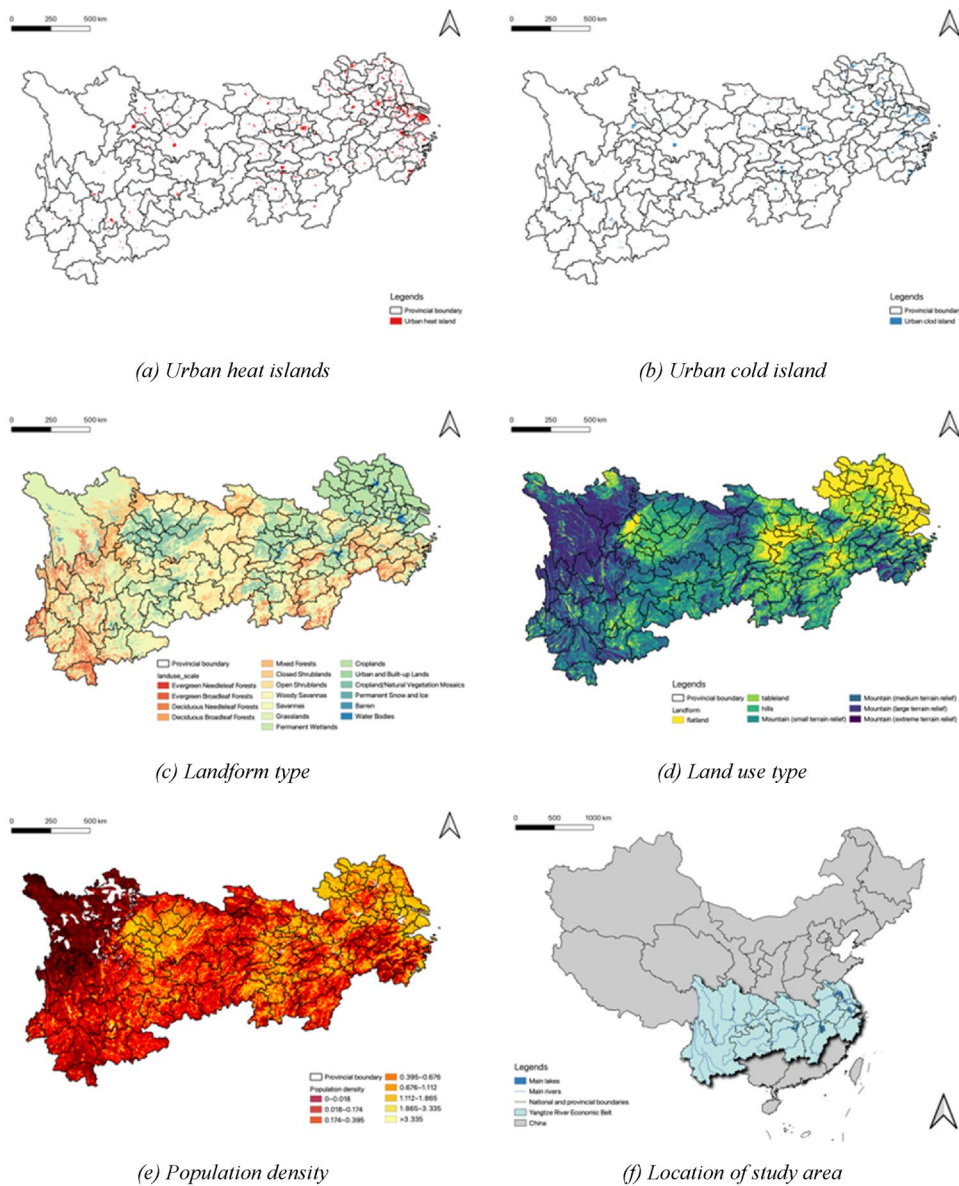
Fig. 1 Flow chart of this study

natural and ecological resources, with complex terrain and climate conditions (Xing et al. 2018). In order to cope with the ecological side effects brought by the rapid economic development and maintain the sustainability of the ecological security pattern, the Chinese government has made great efforts to restore the balance of the river, lake, wetland and forest ecosystems in the region and intended to build it into a demonstration zone for the protection and restoration of the ecological environment system (Luo et al. 2019). Therefore, it is representative that this study takes the Yangtze River Economic Belt as an example to research the relationship between the dynamic changes of city-level spatial pattern of urban blue–green spaces and their cooling effect under the background of ecological restoration.

Data collection and processing

The main datasets used in this study are composed of land use type maps, land surface temperature maps, population distribution maps, and landform type maps (Fig. 2). The spatial scope of all maps is the Yangtze River Economic Belt, including data from 2003 to 2018.[1] The land cover type maps were downloaded from Land Cover Type (MCD12Q1, 500 m) Version 6 data product, which provides global land cover types at yearly intervals (Friedl and Sulla-Menashe 2019). The land surface temperature maps came from MODIS TERRA and AQUA Land

---

[1] Due to the lack of data of 2004 in the dataset of land surface temperature, all the datasets utilized in this work do not include the data of corresponding year.

Fig. 2 Study area and main datasets

(a) Urban heat islands

(b) Urban cold island

(c) Landform type

(d) Land use type

(e) Population density

(f) Location of study area

Surface Temperature (LST) data. These maps provide the spatial distribution of urban heat islands and cold islands, which are defined as the difference in LST of the urban pixels and the non-urban pixels within each urban extent, based on the simplified urban-extent (SUE) algorithm (Chakraborty and Lee 2019). In addition, the dataset not only includes the annual average urban heat island/cold island intensity data from 2003 to 2018, but also provides data from different seasons (winter and summer) and periods (daytime and nighttime). The population distribution maps are derived from WorldPop Global Project Population Data, which provided the estimated residential population per 100×100 m grid square through machine learning approaches (Gaughan et al. 2013). The landform type maps were collected from the Geomorphological Atlas of

the People's Republic of China, in which different types of landforms are represented by integers (Zhou and Cheng 2010).

After data collection, we further clipped the raw raster datasets along the boundary lines of 130 cities within the Yangtze River Economic Belt. The data related to the land use type and urban heat/cold islands was processed with the methods in Chapters 2.3 and 2.4, respectively to obtain the quantitative information reflecting the spatial distribution pattern of urban blue–green spaces and the intensity of urban heat/cold island effect. The remaining parts of the data are processed by calculating the average value of all raster grids in each city to construct the panel dataset of the terrain and population characteristics of 130 cities from 2003 to 2018.

Table 1 Re-classification results of land use types

Original land use type	Re-classified land use type
Evergreen needleleaf forests, evergreen broadleaf forests, deciduous needleleaf forests, deciduous broadleaf forests, mixed forests	Forests
Open shrublands, closed shrublands	Shrublands
Woody savannas, savannas, grasslands	Grasslands
Permanent wetlands, permanent snow and ice, permanent snow and ice	Water bodies
Urban and built-up lands	Urban and built-up lands
Croplands, cropland/natural vegetation, barren	Other lands

Landscape metrics

In this study, we need to quantify the composition and distribution characteristics of urban blue–green spaces at the first step. Here, we introduced the algorithms of landscape metrics to quantify the spatial distribution pattern of urban blue–green spaces. Specifically, the collected land use type maps were clipped into 130 sections according to the boundary lines of cities in the Yangtze River Economic Belt. Then, according to the definition of blue–green space proposed in previous studies (Du et al. 2019; Dzhambov 2018), the original land use type maps were re-classified into six categories (Table 1). Among them, forest, shrublands, grasslands and water bodies were recognized as urban blue–green spaces in this paper.

Finally, three landscape metrics of *PLAND*, *NP* and *LSI*, were utilized to measure the spatial pattern of blue–green spaces at city-level from the perspectives of composition, distribution and shape (Formula 1, 2 and 3).

$$\text{PLAND} = \frac{\sum_{j=1}^{n} a_{ij}}{A} \tag{1}$$

$$\text{NP} = n_i \tag{2}$$

$$\text{LSI} = \frac{0.25 \sum_{k=1}^{n} e_{ik}^*}{\sqrt{A}} \tag{3}$$

where *PLAND* represents the percentage of landscape, which is a fundamental measures of landscape composition; a_{ij} denotes the area of landscape patch j in landscape type i; A denotes the total landscape area; *NP* represents the number of landscape patches of a particular patch type, which is a simple measure of the extent of subdivision or fragmentation of the patch type; n_i denotes the number of patches of the corresponding patch type i; *LSI* represents the total landscape boundary and all edge within the boundary divided by the square root of the total landscape area (square meters) and adjusted by a constant (circular standard for vector layers, square standard for raster). The LSI will increase with increasing landscape shape irregularity or increasing amounts of edge within the landscape. The greater the value of *LSI*, the more complex the shape of the landscape patches; e_{ik}^* denotes total length of edge in landscape between patch types i and k; includes the entire landscape boundary and some or all background edge segments involving class i (McGarigal 2015).

It is worth mentioning that, in general, the landscape metric of NP is sensitive to area. The corresponding NP values of cities with different areas are often affected by the city scale. In the scene where landscape patches can be accurately identified, NP index has certain limitations. However, in this study, because the accuracy of MCD12Q1 V6 is 500 m, the landscape patches with a scale less than 500 m are not able to be accurately identified. Therefore, compared with the selection of PD and other indicators that are not sensitive to the object scale, the use of NP could more truly reflect the spatial distribution pattern (degree of aggregation and dispersion) of various blue–green space patches in different cities for the existing datasets.

Urban heat/cold island effect intensity

In this study, we mainly investigate the influence of the changes on the spatial pattern of urban blue–green spaces on the urban heat/cold island effect to determine its cooling efficiency. Therefore, we introduced the urban heat/cold island data retrieved based on SUE algorithm and MODIS TERRA and AQUA dataset and quantify the intensity of urban heat/cold island effect by calculating the weighted average value of extreme temperature difference they caused (Chakraborty and Lee 2019). The quantification algorithm is presented in Formula 4.

$$\text{Urban heat/cold island effect intensity} = \frac{\sum_{i=1}^{n} t_i a_i}{\sum_{i=1}^{n} a_i} \tag{4}$$

where t_i denotes the land surface temperature difference between the urban heat/cold islands and their surrounding spaces; a_i denotes the area of spaces where the urban heat/cold islands effect being detected. Similarly, we also obtained the data related to the annual average all-day, summer daytime, summer nighttime, winter daytime and winter

Table 2 Descriptive statistics of variables in panel regression model

Type	Variable	Description	Min	Max	Mean
Dependent variables	COLD	Annual average all-day intensity of urban cold island effect	− 1.59	0.00	− 0.85
	WIN_NIG	Annual average winter nighttime intensity of urban cold island effect	− 3.30	0.00	− 0.87
	WIN_DAY	Annual average winter daytime intensity of urban cold island effect	− 5.46	0.00	− 0.99
	SUM_NIG	Annual average summer nighttime intensity of urban cold island effect	− 3.00	0.00	− 0.68
	SUM_DAY	Annual average summer daytime intensity of urban cold island effect	− 3.00	0.00	− 1.06
	HEAT	Annual average all-day intensity of urban heat island effect	0.00	2.64	1.20
Independent variables	F_PLAND	Quantitative results of PLAND index regarding forests	0.00	89.71	15.03
	F_NP	Quantitative results of NP index regarding forests	0.00	1857.00	291.49
	F_LSI	Quantitative results of LSI index regarding forests	0.00	58.85	18.33
	S_PLAND	Quantitative results of PLAND index regarding shrublands	0.00	0.22	0.00
	S_NP	Quantitative results of NP index regarding shrublands	0.00	105.00	2.19
	S_LSI	Quantitative results of LSI index regarding shrublands	0.00	10.82	0.43
	G_PLAND	Quantitative results of PLAND index regarding grasslands	0.52	89.86	47.90
	G_NP	Quantitative results of NP index regarding grasslands	6.00	1796.00	266.62
	G_LSI	Quantitative results of LSI index regarding grasslands	7.21	64.55	24.81
	W_PLAND	Quantitative results of PLAND index regarding water bodies	0.00	32.28	3.11
	W_NP	Quantitative results of NP index regarding water bodies	0.00	256.00	43.54
	W_LSI	Quantitative results of LSI index regarding water bodies	0.00	19.65	6.54
Instrumental variables	U_PLAND	Quantitative results of PLAND index regarding urban and built-up lands	0.00	48.59	3.98
	U_NP	Quantitative results of NP index regarding urban and built-up lands	0.00	316.00	76.59
	U_LSI	Quantitative results of LSI index regarding urban and built-up lands	0.00	20.44	8.71
	POP	Residential population per 100×100 m grid	27.00	38,971.00	4294.29
	GEO	Types of landforms representing by integers[1]	10.95	57.10	31.60

[1]The types of landforms are represented by integers from 0 to 99. The larger the number, the greater the topographic relief and the higher the terrain

nighttime intensity of urban heat/cold island for 130 cities in the Yangtze River Economic Zone from 2003 to 2018, respectively.

Panel regression model

Model construction

To clarify the impact mechanism of the spatial pattern of urban blue–green spaces on their cooling efficiency, this study considers a quantitative explanation with the help of regression models. Since we have obtained a balanced panel dataset of 130 cities in the Yangtze River economic belt from 2003 to 2018 (Table 2) through Sects. "Data collection and processing" ~ "Urban heat/cold island effect intensity", the fixed effect panel regression models are introduced to estimate the relationship between the spatial pattern of urban blue–green spaces and their cooling effect (Formula 5).

$$
\begin{aligned}
y_{it}^{\text{UCI/UHI}} = {} & \beta_1 x_{it}^{\text{forests}} + \beta_2 x_{it}^{\text{shrublands}} + \beta_3 x_{it}^{\text{grasslands}} \\
& + \beta_4 x_{it}^{\text{water}} + \beta_5 x_{it}^{\text{tools}} + \mu_i + \varepsilon_{it}
\end{aligned} \tag{5}
$$

where the dependent variable $y_{it}^{\text{UCI/UHI}}$ could be the annual average all-day, summer daytime, summer nighttime, winter daytime and winter nighttime intensity of urban heat/cold island effect of year t at city i. x_{it}^{forests}, $x_{it}^{\text{shrublands}}$, $x_{it}^{\text{grasslands}}$ and x_{it}^{water} are vectors consisting of calculating results of landscape metrics related to the composition, shape and distribution of four types of urban blue–green spaces of year t at city i. x_{it}^{tools} is a vector consisting of spatial pattern of urban built-up areas and other lands, urban landform and urban population of year t at city i. μ_i denotes the fixed effect term on city i, which varies with the basic natural condition of cities. ε_{it} denotes the error term of year t at city (Yan et al. 2019).

In addition, since the main target of this study is to clarify the relationship between spatial pattern of urban blue–green spaces and their cooling effect with the help of panel regression model, we introduced the F-statistic to estimate the overall validity of the model. Specifically, when running a regression model, the F-statistic provides us with a way for globally testing if any of the independent variables is related to the dependent variables. If the p value associated with the F-statistic is ≥ 0.05: Then there is no relationship between

Fig. 3 TVoE estimating models
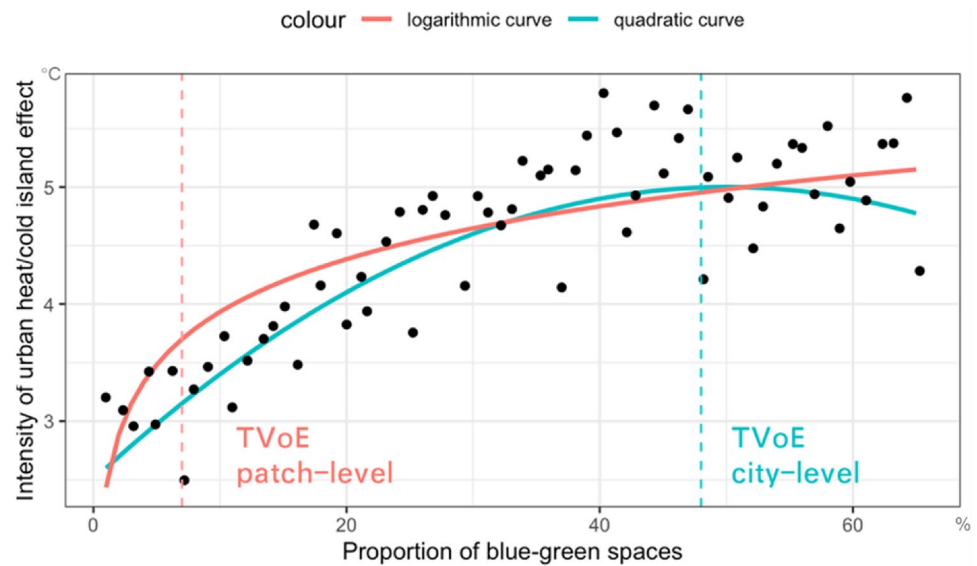
any of the independent variables and dependent variable; if the p value associated with the F-statistic < 0.05: then, at least one independent variable is related to dependent variable (Pope and Webster 1972).

Model pre-estimation

Before running the panel regression model to estimate the relationship between the spatial pattern of urban blue–green spaces and the intensity of urban heat / cold island effect at city level, we need to verify whether the panel dataset constructed in this study meet the input requirements of the model and whether the fixed effect is more suitable for this study scenario.

Stationarity test of variables In the probability theory and statistics, a unit root is a feature of some stochastic processes (such as random walks) that can cause problems in statistical inference involving time series models (Unit root 2021). Therefore, we introduced Levin-Lin-Chu unit root test algorithm to test the stationarity of the original data before panel modeling (Levin et al. 2002). The test results were presented in Appendix 1 and indicated that all time-series data utilized in this study are stationary and could be used for further modeling.

Model selection When using panel data, it is an important question that whether fixed effect model or random effect model would be selected. In this study, we constructed both random and fixed effect models and introduced Hausmann test to determine the model selection (Hausman 1978). The results of Hausmann test are presented in Appendix 2 and further indicated that the fixed effect models are more suitable for global and local scale models constructed to clarify

the relationship between the spatial pattern of urban blue–green spaces and their cooling efficiency.

Quadratic-Curve-Fitting based TVoE estimating model

Previous studies had demonstrated that the cooling effect of blue–green spaces change significantly when the area of certain types of landscape patches exceed a certain value. The threshold value of the cooling efficiency (TVoE) of blue–green space patches is significant to obtain the maximum cooling efficiency (Yu et al. 2018). A Logarithmic-Function-Fitting based TVoE estimation algorithm proposed by Yu et al. (2017) dominated the related research field (Fig. 3). This algorithm based on the marginal effect could obtain the optimal threshold value using logarithmic function to fit the area of landscape patches and its cooling effect. In general, this type of Logarithmic-Function-Fitting based TVoE estimation research is mainly devoted to exploring the optimal cooling efficiency of green patches.

However, we need to re-consider whether the logarithmic function is the most appropriate approach when estimating the cooling efficiency of urban blue–green spaces at city-level. The increase of total area of one type of blue–green space in city inevitably lead to the decrease of other types. As a result, the cooling efficiency of the blue–green spaces may not increase monotonously with the change of size, shape or spatial distribution. Therefore, a TVoE estimating algorithm based on quadratic curve is proposed in this study (Fig. 3). Specifically, we fit the relationship between the spatial pattern of blue–green spaces and the intensity of urban heat/cold island effect with quadratic function and define the point of local extreme value of quadratic function as TVoE at city level. In general, this type of Quadratic-Curve-Fitting

based TVoE estimating model is proposed to calculate the overall composition and distribution pattern of various blue–green spaces in cities with ideal cooling effect at city-level.

Results

Impact mechanism of the spatial pattern of urban blue–green spaces on its cooling efficiency

After the pre-test estimation, the impact of the city-level spatial pattern of urban blue–green spaces on their cooling efficiency was revealed in fixed effect regression models under various scales.

Global scale

Firstly, we constructed fixed effect models which took the annual average all day heat/cold island intensity as the dependent variables to examine the overall relationship between the spatial pattern of urban blue–green spaces and their cooling efficiency at city-level. The results are presented in Table 3.

The output of the models indicated that the proportion and distribution characteristics of forests and shrublands in urban space have significant impacts on the intensity of urban cold island effect. Specifically, the intensity of urban cold island effect can be enhanced by 0.013 ℃ and 6.837 ℃ respectively when the proportion of forests and shrublands increases by 1% (PLAND index increases by 1 unit). At the same time, the more concentrated the distribution of shrublands (NP index decreased by 1 unit), the greater the intensity of urban cold island effect (0.007 ℃).

Besides, this study also found that the cooling effect of urban blue–green space on urban cold island and heat island has significant difference. Specifically, the proportion and distribution of forests and shrublands which showed significant impacts on the intensity of urban cold island effect could not mitigate the urban heat island effect significantly. Grasslands and water bodies are the key factors to deal with urban heat island. The intensity of urban heat island effect can be alleviated by 0.005 ℃ and 0.019 ℃, respectively when the proportion of grasslands and water bodies increases by 1% (PLAND index increases by 1 unit). The more scattered the distribution of shrublands (NP index increased by one unit), the weaker the intensity of urban heat island effect (0.007 ℃).

These results preliminarily proved that the spatial pattern of urban blue–green space at city-level has significant cooling effect. In addition to alleviating the urban heat island effect, which had been illustrated in previous studies, it can also enhance the urban cold island effect. Therefore, this

Table 3 Outputs of global panel regression models

Variables	COLD		Heat	
	Estimate	t value	Estimate	t value
Forests				
F_PLAND	− 0.0136**	− 2.379	− 0.0008	− 0.297
F_NP	− 0.0001	− 0.611	0.0000	0.3933
F_LSI	− 0.0002	− 0.02	− 0.0034	− 0.743
Shrublands				
S_PLAND	− 6.8371***	− 5.049	− 0.2356	− 0.351
S_NP	0.0069**	2.1385	0.0014	0.88
S_LSI	0.0044	0.1952	− 0.0021	− 0.185
Grasslands				
G_PLAND	− 0.0024	− 0.799	− 0.0053***	− 3.551
G_NP	0.0001	0.2596	− 0.0004***	− 3.395
G_LSI	0.0108	1.4544	0.0056	1.5335
Waterbodies				
W_PLAND	0.0006	0.0336	− 0.0185*	− 1.9426
W_NP	0.0002	0.1677	0.0001	0.2277
W_LSI	0.0045	0.3763	− 0.0075	− 1.274
Instrument variables				
U_PLAND	− 0.0072	− 0.625	0.0140**	2.453
U_NP	− 0.0014	− 0.955	0.0010	1.4079
U_LSI	0.0252	0.9727	0.0004	0.0291
POP	0.0000	1.2423	0.0000**	− 2.227
GEO	− 0.0495	− 0.215	− 0.0404	− 0.354
F-statistic				
Statistics	2.411850		3.249170	
p value	0.001027		0.000008	

*Means $0.05 < p$ value < 0.1

**Means $0.01 < p$ value < 0.05

***Means p value < 0.01

study will move another step to reveal the heterogeneity in the impact mechanisms of urban blue–green spaces on the intensity of urban cold island effect.

Temporal heterogeneity

We constructed four fixed effect models which took the summer daytime, summer nighttime, winter daytime and winter nighttime urban cold island intensity as the dependent variables to reveal the differences within the impacts of city-level spatial pattern of urban blue–green spaces on urban cold islands in various time periods. The results are presented in Table 4.

The outputs of the models showed that some spatial pattern attributes of urban blue–green space at city-level, which are not related to the all-day intensity of urban clod islands effect, showed extra significant impacts on that of specific time periods. Specifically, in addition to the size, the city-level distribution and shape of the forest will

Table 4 Outputs of local panel regression models (temporal heterogeneity)

Variables	Winter night		Winter day		Summer night		Summer day	
	Estimate	t value	Estimate	t value	Estimate	t value	Estimate	t value
Forests								
F_PLAND	− 0.0034	− 0.4651	− 0.0189***	− 2.5873	0.0048	0.5373	− 0.0131	− 1.496
F_NP	− 0.0004	− 1.6057	0.0008***	2.9703	0.0004	1.2948	0.0006**	2.0363
F_LSI	0.0175	1.4908	− 0.0261**	− 2.2382	− 0.0222	− 1.535	− 0.0372***	− 2.648
Shrublands								
S_PLAND	− 7.7666***	− 4.4575	− 3.0110*	− 1.7389	0.5863	0.2738	− 4.6447**	− 2.2324
S_NP	0.0095*	2.2854	0.0051	1.2487	− 0.0047	− 0.9183	0.0086*	1.74
S_LSI	− 0.0182	− 0.6308	− 0.0256	− 0.8911	− 0.0439	− 1.2355	− 0.0098	− 0.284
Grasslands								
G_PLAND	− 0.0006	− 0.1583	− 0.0058	− 1.5096	− 0.0004	− 0.0938	− 0.0058	− 1.2687
G_NP	0.0005	1.6397	0.0003	1.0924	0.0004	1.2254	− 0.0001	− 0.2031
G_LSI	− 0.0119	− 1.2457	0.0119	1.2564	− 0.0069	− 0.5892	0.0157	1.3741
Water bodies								
W_PLAND	− 0.0070	− 0.2809	0.0073	0.2962	− 0.0155	− 0.5078	− 0.0533*	− 1.8004
W_NP	− 0.0005	− 0.3193	0.0012	0.7479	0.0043**	2.172	0.0042**	2.2052
W_LSI	0.0222	1.4497	− 0.0197	− 1.2936	− 0.0268	− 1.4218	− 0.0590***	− 3.2226
Instrument variables								
U_PLAND	0.0283**	1.9115	− 0.0177	− 1.1998	0.0286	1.5705	0.0217	1.2277
U_NP	0.0018	0.9394	− 0.0019	− 0.9872	− 0.0012	− 0.5154	− 0.0049**	− 2.1195
U_LSI	− 0.0166	− 0.4965	0.0631*	1.9028	0.0202	0.4918	0.0582	1.4614
POP	0.0000	0.6303	0.0000	− 0.3305	0.0000	0.5977	0.0000	− 1.3939
GEO	0.0952	0.3213	0.0857	0.291	− 0.1895	− 0.5203	0.2543	0.7187
F-statistic								
Statistics	2.590840		2.605750		1.756850		2.940870	
p value	0.000380		0.000349		0.028253		0.000050	

*Means $0.05 < p$ value < 0.1

**Means $0.01 < p$ value < 0.05

***Means p value < 0.01

also affect the daytime urban cold island. The daytime intensity of urban cold island effect in winter and summer can be enhanced by 0.0008 ℃ and 0.0006 ℃, respectively when the distribution of forests gets more concentrated (NP index decreased by 1 unit). Similarly, as the shape of the forests becomes more complex (LSI index increased by 1 unit), the intensity of urban cold island effect in the two seasons can be enhanced by 0.026 ℃ and 0.037 ℃, respectively. Water body has also been proved to be significantly associated with winter urban cold island effect. The larger the area, the more concentrated the distribution, and the more complex the shape of water bodies, the higher the intensity of urban cold island effect. The UCI intensity increased by 0.053 ℃, 0.004 ℃ and 0.059 ℃, respectively for one unit change in PLAND (+), NP (−) and LSI (+) indices of water bodies at city-level.

Moreover, the results from Table 4 also indicated that the city-level spatial pattern of blue–green space is more closely related to urban cold island effect in summer and daytime. Specifically, compared with other seasons and time periods, the spatial patterns of water bodies and forests of urban blue–green spaces at city-level have additional effects on the urban cold island effect in summer and daytime, respectively.

Spatial heterogeneity

As the cooling effect of the blue–green spaces changes with the characteristics of the regional natural environment and the intensity of human activities, in order to eliminate the errors caused by these spatial factors on the regression results, we divided the 130 prefecture level cities in the dataset into 4 sections according to the terrain conditions and the permanent population density.[2] Each

[2] The division is based on whether the values of POP and GEO variables regarding provinces exceed the average value.

Table 5 Outputs of local panel regression models (spatial heterogeneity)

Variables	POP (+) regions		POP (−) regions		GEO (+) regions		GEO (−) regions	
	Estimate	t value	Estimate	t value	Estimate	t value	Estimate	t value
Forests								
F_PLAND	− 0.0060	− 0.9039	− 0.0151	− 1.5005	− 0.0170*	− 1.7922	− 0.0003	− 0.0307
F_NP	− 0.0001	− 0.4463	− 0.0001	− 0.1795	− 0.0002	− 0.7705	0.0002	0.4201
F_LSI	0.0010	0.0969	− 0.0083	− 0.5212	− 0.0002	− 0.0126	0.0009	0.0597
Shrublands								
S_PLAND	− 1.3730	− 0.503	− 8.5307***	− 4.3673	− 7.0319***	− 4.8418	− 8.6988	− 0.5402
S_NP	− 0.0049	− 0.3369	0.0099**	2.1805	0.0081**	2.2369	0.0990	0.6889
S_LSI	− 0.0061	− 0.2193	− 0.0171	− 0.4207	− 0.0091	− 0.3295	− 0.0671	− 0.4023
Grasslands								
G_PLAND	− 0.0026	− 0.8914	0.0076	1.1085	− 0.0032	− 0.4854	− 0.0009	− 0.255
G_NP	0.0002	0.955	− 0.0001	− 0.1164	− 0.0001	− 0.2172	0.0003	0.8002
G_LSI	− 0.0090	− 1.1591	0.0374**	2.416	0.0200*	1.873	− 0.0037	− 0.332
Water bodies								
W_PLAND	− 0.0007	− 0.028	0.0112	0.376	0.0502	0.7053	− 0.0186	− 0.9147
W_NP	0.0011	0.9213	− 0.0003	− 0.122	0.0026	1.3058	− 0.0017	− 1.0116
W_LSI	0.0000	− 0.0008	0.0045	0.2293	− 0.0099	− 0.6346	0.0138	0.5386
Instrument variables								
U_PLAND	− 0.0042	− 0.4196	− 0.0458	− 1.4362	− 0.0401*	− 1.7744	0.0137	0.9341
U_NP	0.0004	0.3309	− 0.0052	− 1.1933	− 0.0003	− 0.1509	− 0.0033	− 1.4552
U_LSI	− 0.0074	− 0.2833	0.0828	1.5882	0.0083	0.198	0.0551	1.52
POP	0.0000	0.755	0.0000	− 0.5427	0.0000**	2.1364	0.0000	− 0.0967
GEO	− 0.3759	− 1.5244	0.1825	0.474	0.4641	1.3143	− 0.4678	− 1.5263
F-statistic								
Statistics	1.181320		2.050950		2.554060		0.706551	
p value	0.272940		0.007270		0.000524		0.798220	

*Means $0.05 < p$ value < 0.1

**Means $0.01 < p$ value < 0.05

***Means p value < 0.01

section contains 65 provinces, which represent the regions with large population (POP+), sparse population (POP−), mountain topography (GEO+) and flatland topography (GEO−), respectively. Then, we constructed 4 fixed effect models which took the annual all-day urban cold island intensity as the dependent variables in these four regions to further detect the spatial heterogeneity within the impacts of city-level spatial pattern of urban blue–green spaces on urban cold islands. The results were presented in Table 5.

The outputs of the models showed that additional links between the shape of grasslands and urban cold island exist in regions with specific demographic and topographical characteristics. In detail, as the shape of the grasslands at city-level in sparsely populated regions and mountainous regions becomes more complex (LSI index increased by 1 unit), the intensity of urban cold island effect can be enhanced by 0.037 ℃ and 0.020 ℃, respectively.

In addition, the results from Table 5 further demonstrated that the impact of city-level spatial pattern of blue–green

spaces on the intensity of urban cold island is more significant in sparsely populated regions and mountainous regions. Specifically, the size, distribution and shape of various types of urban blue–green spaces, such as forests, shrublands and grasslands, significantly affect the urban cold island in sparsely populated (POP-) regions and mountainous (GEO+) regions. On the contrary, there was no statistically significant (p value > 0.1) relationship with the UCI in populated regions and flatland regions.

Threshold effect (TVoE) estimation of the cooling efficiency

After clarifying the impact of city-level spatial pattern of blue–green spaces on urban cold island effect, we turned to investigate the optimal spatial pattern of blue–green spaces with the maximum cooling efficiency at city scale. Specifically, we use the Quadratic-Curve-Fitting based TVoE estimating model proposed in chapter 2.6 to fit the relationship between the PLAND, NP and LSI indexes of the 4 types
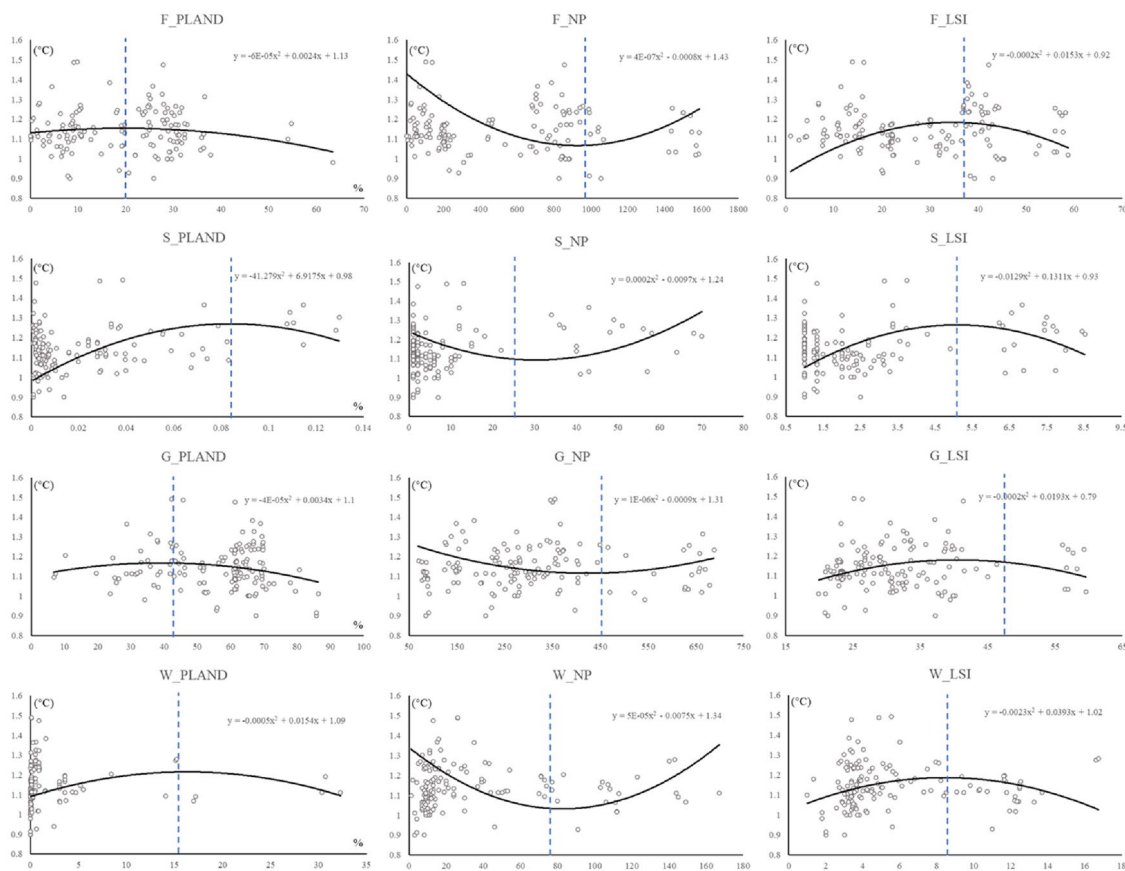
Fig. 4 Estimation results of TVoE

of blue–green space (forests, shrublands, grasslands, water bodies) and the intensity of urban cold island effect. The results were shown in Fig. 4.

The fitting results showed that, being similar to the logarithmic function, the quadratic function is also suitable for fitting the relationship between the spatial characteristics of blue–green space and its cooling effect. Different from logarithmic fitting, the 12 fitting functions constructed in this study do not show monotonic increasing or decreasing characteristics, and the vertices are identified in the corresponding domains. This further indicated that different perspectives and methods should be utilized to estimate the TVoE in cooling efficiency of blue–green spaces from patch-level and city-level, respectively. As mentioned in chapter 2.6, the cooling effect of blue–green patches always increases with area theoretically. Therefore, when estimating the TVoE at patch-level, we focus on finding the turning point where the increasing rate of cooling efficiency slows down and define it as the threshold point (Yu et al. 2017). However, when re-examining from the perspective of the whole city, it can be found that the city-level blue–green space system will change accordingly when the area, distribution and shape of one type of blue–green space in cities change. Therefore,

combined with the present hypothesis and the fitting results in Fig. 4, we supposed that when estimating the TVoE of blue–green spaces at city-level, we should turn to find out the change points regarding four types of urban blue–green spaces where the changing direction of the intensity of urban cold island effect change.

The fitting results indicated that the intensity of urban cold island effect first increased and then decreased with the expand of area and the complex of shape of urban blue–green spaces at city-level. Specifically, on the one hand, the intensity of urban cold island effect reaches the local maximum (1.20 °C) when the area ratio of forests, shrublands, grasslands and water bodies is about 20%, 0.1%, 42.5% and 15.4%, respectively. On the other hand, when the LSI index of forests, shrublands, grasslands and water bodies at city level reach 38.25, 5.08, 48.25 and 8.54 respectively, the intensity of urban cold island effect reaches another local maximum (1.23 °C). In contrast, the relationship between the city-level distribution of urban blue–green spaces and urban cooling island showed a different trend. The intensity of urban cold island effect first decreased and then increased with the discretization of urban blue–green spaces at city-level. Specifically, when the NP index of forests, shrublands,

grasslands and water bodies at city level reach 1000, 24.25, 450 and 75 respectively, the intensity of urban cold island effect reaches another local minimum (1.08 ℃). This further showed that when the blue–green space in the city presents an extreme aggregation and discrete distribution pattern, it is conducive to play its cooling effect.

In summary, by using the Quadratic-Curve-Fitting based TVoE estimating model designed in this study to fit the cold island effect efficiency of urban blue–green space, it is found that the relationship between cooling efficiency of urban blue–green space and its city-level spatial distribution showed a significant threshold effect. Combined with this TVoE model and landscape pattern indices, the optimal spatial pattern of urban blue–green spaces at city-level (from the aspects of area, shape and distribution) with the best cooling efficiency could be proposed.

Discussions

Combining the calculation results of the panel regression models and the Quadratic-Curve-Fitting based TVoE model constructed in "Results", this study has basically given answers the two research questions raised in the introduction section.

On the one hand, the results evidenced that the proportion and distribution characteristics of forests and shrublands in urban areas improved the intensity of urban cold island effect significantly, while that of grassland and water bodies mitigated urban heat island effect. Moreover, it was demonstrated that the city-level spatial pattern of urban blue–green space has a greater influence on its cooling efficiency at specific time periods (summer and daytime) and regions (mountainous cities with a small population).

On the other hand, it was also estimated that the cooling effect reaches the local maximum (around 1.2 ℃) when the PLAND / LSI index of forests, shrublands, grasslands, and water bodies at city-level is about 20%, 0.1%, 42.5% and 15.4%/38.25, 5.08, 48.25 and 8.54, respectively. Furthermore, when the NP index of forests, shrublands, grasslands and water bodies at city level reach 1000, 24.25, 450 and 75 respectively, the intensity of urban cold island effect reaches another local minimum (1.08 ℃). The results of the above threshold calculations provide an important reference for the optimal spatial pattern of blue–green spaces of the maximum cooling efficiency at city scale.

Therefore, in this section, we further discussed the reasonings for these findings. Specifically, we deeply discussed the explanations on the influence mechanism and the validity of Quadratic-Curve-Fitting based TVoE estimating model. The details contents are as follows.

Explanations on the influence mechanism

Overall relationship between urban blue–green spaces and their cooling efficiency

The results of global models (Table 3) explicitly delineated that the 4 types of urban blue–green spaces (forests, shrublands, grasslands, waterbodies) all have significant cooling effect, which is consistent with previous findings (Yang et al. 2017). However, the four landscape elements have notable different ways to achieve cooling. Specifically, grasslands and water bodies are the main driving factors to alleviate urban heat island intensity, and the intensity of urban cold island effect changes with the spatial pattern of forests and shrubland at city-level.

This might be closely related to the difference of light transmittance in different types of blue–green spaces. Compared with grasslands and water bodies, the canopy of forests and shrublands is closed and the structure is complex, which makes the light intensity in the space decrease significantly. The decrease of light energy input helps to reduce the temperature, which leads to the obvious difference of cooling principle between different types of blue–green spaces (Tang et al. 2009; Chen et al. 2015).

In general, regions with significant vegetation cover, such as forests and shrublands, could effectively improve surface moisture, heat capacity and thermal inertia due to their high latent heat flux. Therefore, the spatial pattern of these two types of blue–green spaces is the key to maintain the efficient operation of urban Cold Island. On the contrary, grasslands and water bodies are more sensitive to heat exchange because they have no vegetation cover, so they have a greater impact on urban heat island. The spatial morphology planning of blue–green infrastructure are also considered as important roles in improving urban resilience and achieving sustainable goals for urban environment.

Spatial–temporal heterogeneity in the impact mechanism

Temporal heterogeneity The results of local models (Table 4) illustrated that the impact of spatial pattern of blue–green spaces at city-level on the urban cold island effect varies with time, and the urban blue–green space has a greater influence on urban cold island in summer and daytime. Specifically, we took the distribution characteristics of urban cold island of Shanghai (Fig. 5) in different seasons (summer and winter in 2018) and time periods (daytime and nighttime) as examples to try to explain the temporal heterogeneity of the cooling effect of blue–green spaces.

From the distribution of urban cold islands in Shanghai in 2018, it was found that the urban cold islands in summer and daytime have the characteristics of more quantity, wide distribution and small area compared with those in winter
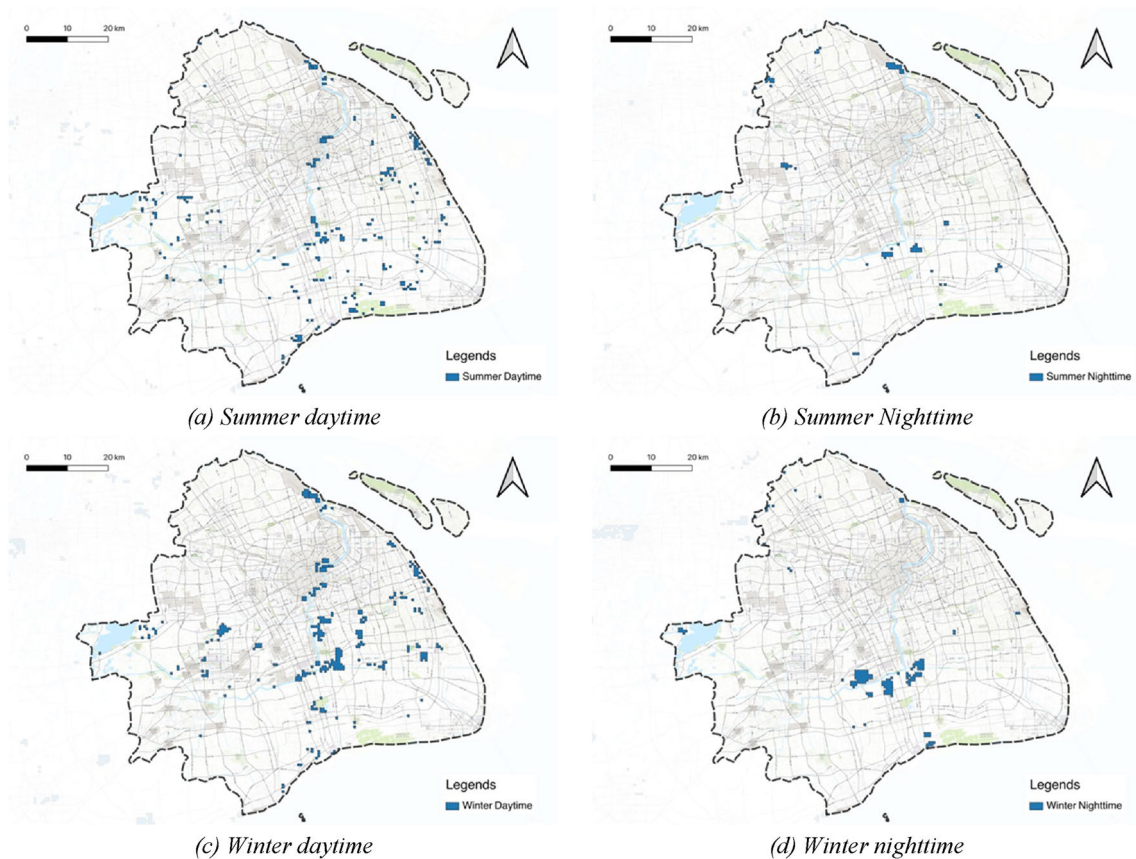
(a) Summer daytime

(b) Summer Nighttime

(c) Winter daytime

(d) Winter nighttime

Fig. 5 Urban cold island in Shanghai (2018)

Table 6 Attributes of urban cold islands in Shanghai (2018)

Season	Mean area (km^2)	Amount	Time period	Mean area (km^2)	Amount
Summer	0.6356	188	Daytime	0.7311	271
Winter	1.1864	141	Nighttime	1.5282	58

and nighttime. The average area of urban cold islands in summer and daytime were only 0.6356 and 0.7311 km^2, while the average area of which reach 1.1864 and 1.5282 km^2 respectively in winter and nighttime. Similarly, the number of urban cold islands in summer and daytime is 47 (188/141) and 213 (271/58) more than those in winter and nighttime, respectively (Table 6).

This illustrated that the reasonable spatial pattern of urban blue–green space at city-level (especially forests and water bodies) could effectively promote the cooling effect of evenly distributed and small area urban cold islands but showed no effect on centralized and large area ones.

Spatial heterogeneity The results of local models (Table 5) further illustrated that the link between the city-level spatial pattern of urban blue–green spaces and urban cold island effect only existed in mountainous cities with a small population (POP− and GEO+). The special natural conditions,

urban spatial structure, and traffic mode of such cities may be the factors for urban blue–green space to play the initial role.

Firstly, the climate environment of mountain cities with low population density is significantly affected by mountain-valley breezes (Zeng and Tian 2013). The phenomenon of mountain-valley breezes is considered to be the main reason for the rise of urban temperature and humidity (Cao and Xiao 2013). Therefore, we could infer from the results of the spatial heterogeneity that the change of urban blue–green spatial pattern at city-level might be an important factor affecting mountain-valley breezes. Rational allocation of urban blue–green space (especially shrublands and grasslands) is one of the effective strategies to suppress mountain-valley breezes and improve urban cold island effect.

Secondly, mountainous cities with low population density are restricted by their terrain conditions, and its urban spatial
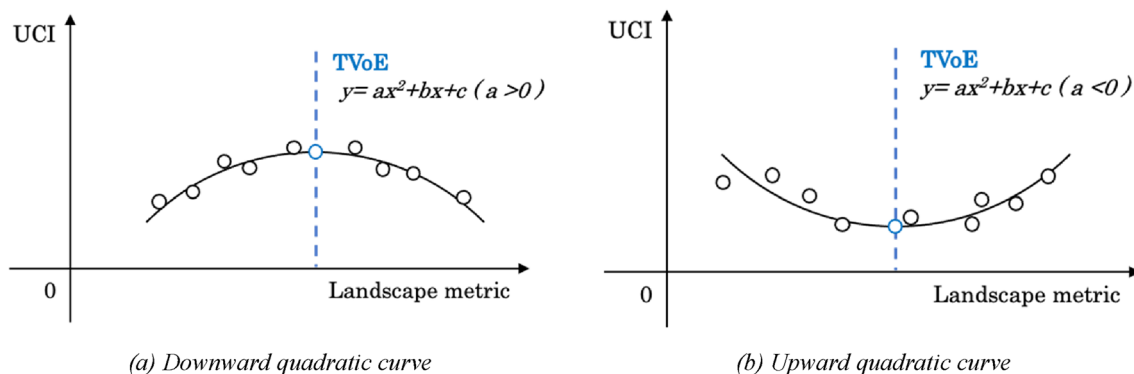
(a) Downward quadratic curve　　　*(b) Upward quadratic curve*

Fig. 6 Basic forms of Quadratic-Curve-Fitting based TVoE estimating model

structure mainly developed into 'group mode', which is different from that of big cities in plain area ('core mode'). To a certain extent, the multi-core development model avoids the aggregation of urban resources, economy and industry (Huang 2005). Therefore, we could infer from the results of the spatial heterogeneity that the development mode of uniform allocation of urban resources and optimal urban blue–green space allocation could maximize the cooling effect.

Thirdly, mountainous cities with low population density are subject to the geographical environment, and most of the urban roads follow the terrain and mountains and connect with the main roads in a zigzag way, which makes the vehicles driving difficult. This is the reason why cars need to make sharp turns and accelerate and decelerate more frequently. This kind of transportation mode helps to reduce the total amount of resident's transportation and increase the utilization of public transportation (Zeng and Tian 2013). Therefore, we could infer from the results of the spatial heterogeneity that it is also an important means to improve the cooling efficiency of urban blue–green spaces by reducing traffic and alleviating vehicle energy consumption and exhaust emissions.

Application of Quadratic-Curve-Fitting based TVoE estimating model

Using the Quadratic-Curve-Fitting based TVoE estimating model proposed in "Quadratic-Curve-Fitting based TVoE estimating model", we fit the relationship between the urban cold island effect and the spatial pattern of urban blue–green spaces and estimate the TVoE and optimal pattern of the urban blue–green spaces at city-level. The results in Sect. 3.3 further delineated that the model has good performance. The global blue–green space pattern with the maximum cooling efficiency could be estimated from three aspects of area, distribution and shape. Specifically, additional focus should be paid on the two following points when utilizing this model:

On the one hand, the Quadratic-Curve-Fitting based TVoE estimating model is specifically designed to estimate

the optimal spatial pattern of urban blue–green spaces at city-level. Mainstream Logarithmic-Function-Fitting based TVoE estimating models are mainly used to estimate the size threshold of the cooling efficiency of landscape patches (Peng et al. 2020), that is, to calculate the corresponding area when the cooling efficiency of a single urban green space or water body is the maximum (Fig. 3). In these studies, landscape patches are assumed to exist independently. Therefore, its cooling capacity will increase monotonously with the increase of its area, theoretically. However, when investigating from city-level, the area, distribution and shape of all kinds of urban blue–green spaces will be influenced by other kinds. For example, the increase of the area of one kind of blue–green space will inevitably compress the area of other kinds of spaces in the city. Based on this, the proposed model is designed to estimate the global optimal pattern of a city's blue–green space from an overall perspective.

On the other hand, there are two main forms of the outputs of the Quadratic-Curve-Fitting based TVoE estimating model. In this study, a quadratic function ($y = ax^2 + bx + c, a \neq 0$) was utilized to fit the landscape metrics corresponding to the urban blue–green spatial pattern and the intensity of urban cold island effect under the corresponding spatial pattern. Therefore, the fitting functions were classified into two categories (Fig. 6).

In cases that the graph of fitted function opens upwards, the overall intensity of urban cold island reaches the highest (local maximum of function) when the landscape metric corresponding to spatial pattern of urban blue–green spaces equals to the vertex value (i.e., the axis of symmetry) of the parabola of the univariate quadratic function. As the landscape metrics are further away from vertex, the intensity of urban Cold Island will gradually decrease. On the contrary, in other cases that the graph of fitted function opens downwards, the overall intensity of urban cold island reaches the lowest (local minimum of function) when the landscape metric corresponding to spatial pattern of urban blue–green spaces equals to the vertex value. As the landscape metrics are further away from vertex, the intensity of urban Cold Island gradually

increased. For instance, in the case study of this work, the fitting results of the relationship between area and shape of urban blue–green spaces and urban cold island intensity are, respectively, consistent with the above two scenarios.

In summary, the threshold value of urban blue–green spaces' cooling effect could be estimated at the vertex of quadratic function by using the model proposed in this study, but the meaning of the threshold value needs to be further discussed with reference to the fitting results (parameter *a* in the quadratic function).

Conclusions

In this study, we clarified the relationship between the urban blue–green spaces and urban cold island effect from the global scale and investigate the spatial–temporal heterogeneity within it. Then, we also proposed a Quadratic-Curve-Fitting based TVoE estimating model and further estimated the threshold value and optimal spatial pattern of urban blue–green spaces at city-level. From a case study established in the Yangtze River Economic Belt, China, the main conclusions are listed as follows.

First, spatial pattern of urban blue–green spaces at city-level has noticeable cooling effect. The proportion and distribution characteristics of forests and shrublands in urban space have significant impacts on the intensity of urban cold island effect. Specifically, the intensity of urban cold island effect can be enhanced by 0.013 ℃ and 6.837 ℃ respectively when the proportion of forests and shrublands increases by 1% (PLAND index increases by 1 unit). At the same time, the more concentrated the distribution of shrublands (NP index decreased by 1 unit), the greater the intensity of urban cold island effect (0.007 ℃).

Second, the impact of spatial pattern of blue–green spaces at city-level on the urban cold island effect varies with time and space. Specifically, the city-level spatial pattern of blue–green space is more closely related to urban cold island effect in summer and daytime. Moreover, the link between the urban blue–green spaces and urban cold island effect only existed in mountainous cities with a small population.

Third, there is a noticeable threshold effect between spatial pattern of blue–green spaces at city-level and the global urban cold island effect intensity. Specifically, the intensity of urban cold island effect first increased and then decreased with the expand of area and the complex of shape of urban blue–green spaces at city-level. In contrast, it first decreased and then increased with the discretization of urban blue–green spaces. The global average intensity of urban cold island effect reaches the local maximum (1.20~1.23 ℃) when the area ratio/LSI index of forests, shrublands, grasslands, and water bodies is about 20%, 0.1%, 42.5% and 15.4%/38.25, 5.08, 48.25 and 8.54, respectively. Furthermore, when the NP index of forests, shrublands, grasslands

and water bodies at city level reach 1000, 24.25, 450 and 75 respectively, the intensity of urban cold island effect reaches another local minimum (1.08 ℃).

Based on the above conclusions, we put forward the following policy implications and suggestions for planning of blue–green infrastructure for the urban heat and cooling island effect. When making urban planning and ecological planning with urban blue–green infrastructure as the main object, it is necessary to coordinate the layout mode of all categories of blue–green spaces from a macro perspective. In addition to combating the negative effects of climate change, ecological lands, represented by blue–green spaces, also have great potential to increase urban resilience. Furthermore, in order to maximize the ecological benefits, the natural geography and social economic characteristics of the target city should be taken into consideration during the planning procedure. In addition, there are significant differences in cooling effect and cooling principle between different categories of urban blue–green space. When using ecological lands to adjust urban micro-climate, we need to combine local climate zone to determine the most optimal blue–green space adjustment scheme to achieve the sustainable development goals for urban environment.

The most important contribution of this paper might be that we clarified the relationship between urban blue–green spaces and urban cold island effect at city-level based on the empirical evidence. To our knowledge, this is the first empirical study to explore the link between the city-wide proportion, distribution and shape characteristics of various types of ecological lands (forests, shrublands, grasslands and water bodies) and the overall intensity of the cold island effect at city-level. The empirical results of this study evidenced that, in addition to the characteristics of patches, the overall spatial pattern of urban blue–green space will also significantly affect its cooling effect. Optimal regulation of urban ecological lands is another key factor to mitigate urban heat island and promote urban Cold Island in the future. Additionally, the Quadratic-Curve-Fitting based TVoE estimating model proposed in this work, which is inspired from the Logarithmic-Function-Fitting based models designed for patch-level research (Yu et al. 2017), could also contribute to estimate the threshold effect and optimal spatial pattern of urban blue–green spaces at city-level.

However, due to the lack of data, the resolution of the original land use data set (MCD12Q1) used to quantify the spatial pattern of urban blue–green space is 500 m, and the accuracy of the quantitative results still have room to improve. This is the main deficiency of this study and the compromise of large-scale spatial research. In the future, the main research direction is to select more accurate data and methods to investigate the mechanisms of the heterogeneity of the impact of urban blue–green spatial pattern on its global cooling efficiency.

Appendix 1

See Table 7.

Table 7 Results of unit root test

Variable	z value	p value	Result
F_PLAND	− 5.2357	8.22E−08	Stationarity
F_NP	− 14.573	2.20E−16	Stationarity
F_LSI	− 10.73	2.20E−16	Stationarity
S_PLAND	− 29.726	2.20E−16	Stationarity
S_NP	− 22.893	2.20E−16	Stationarity
S_LSI	− 25.94	2.20E−16	Stationarity
G_PLAND	− 1.1279	1.30E−01	Stationarity
G_NP	− 17.222	2.20E−16	Stationarity
G_LSI	− 17.5	2.20E−16	Stationarity
W_PLAND	− 16.417	2.20E−16	Stationarity
W_NP	− 15.174	2.20E−16	Stationarity
W_LSI	− 20.269	2.20E−16	Stationarity
U_PLAND	− 21.102	2.20E−16	Stationarity
U_NP	− 157.47	2.20E−16	Stationarity
U_LSI	− 56.008	2.20E−16	Stationarity
POP	− 9.1842	2.20E−16	Stationarity
GEO	− 27.576	1.00E+00	Stationarity
COLD	− 23.908	2.20E−16	Stationarity
HEAT	− 27.214	2.20E−16	Stationarity
WIN DAY	− 33.065	2.20E−16	Stationarity
WIN NIG	− 43.277	2.20E−16	Stationarity
SUM DAY	− 23.361	2.20E−16	Stationarity
SUM NIG	− 51.123	2.20E−16	Stationarity

Appendix 2

See Table 8.

References

Antoszewski P, Świerk D, Krzyżaniak M (2020) Statistical review of quality parameters of blue–green infrastructure elements important in mitigating the effect of the urban heat island in the temperate climate (C) zone. Int J Environ Res Public Health 17(19):7093

Byrne J, Yang J (2009) Can urban greenspace combat climate change? Towards a subtropical cities research agenda. Aust Plan 46(4):36–43

Cao K, Xiao J (2013) Road system planning based on topographic analysis: case studies of mountainous cities in southwest China. Mt Res 31(4):473–481

Carvalho D, Martins H, Marta-Almeida M, Rocha A, Borrego CJUC (2017) Urban resilience to future urban heat waves under a climate change scenario: a case study for Porto urban area (Portugal). Urban Clim 19:1–27

Chakraborty T, Lee X (2019) A simplified urban-extent algorithm to characterize surface urban heat islands on a global scale and examine vegetation control on their spatiotemporal variability. Int J Appl Earth Obs Geoinf 74:269–280

Chen R, You XY (2019) Reduction of urban heat island and associated greenhouse gas emissions. Mitig Adapt Strat Global Change 25:1–23

Chen X, Li L, Wang J (2015) Heat island effect mitigation by urban green space system: a case study of Taizhou city. Ecol Environ Sci 24:643–649

Du H, Song X, Jiang H, Kan Z, Wang Z, Cai Y (2016) Research on the cooling island effects of water body: a case study of Shanghai, China. Ecol Ind 67:31–38

Table 8 Results of Hausmann test

Model	Chi-Sq	df	p value	Result of model selection
COLD ~ Landscape	116.49	17	2.20E−16	Fixed effect model
HEAT ~ Landscape	161.12	17	2.20E−16	Fixed effect model
WIN_NIG ~ Landscape	41.213	17	8.70E−04	Fixed effect model
WIN_DAY ~ Landscape	55.518	17	5.66E−06	Fixed effect model
SUM_NIG ~ Landscape	44.217	17	3.18E−04	Fixed effect model
SUM_DAY ~ Landscape	76.059	17	1.91E−09	Fixed effect model
POP_UP ~ Landscape	24.054	17	1.18E−01	Fixed effect model
POP_DOWN ~ Landscape	50.726	17	3.26E−05	Fixed effect model
GEO_UP ~ Landscape	262.02	17	2.20E−16	Fixed effect model
GEO_DOWN ~ Landscape	27.64	17	4.93E−02	Fixed effect model

Du H, Cai Y, Zhou F, Jiang H, Jiang W, Xu Y (2019) Urban blue–green space planning based on thermal environment simulation: a case study of Shanghai China. Ecol Indic 106:105501

Dzhambov AM (2018) Residential green and blue space associated with better mental health: a pilot follow-up study in university students. Arch Ind Hyg Toxicol 69(4):340–349

Estoque RC, Murayama Y, Myint SW (2017) Effects of landscape composition and pattern on land surface temperature: an urban heat island study in the megacities of Southeast Asia. Sci Total Environ 577:349–359

Friedl M, Sulla-Menashe D (2019) MCD12Q1 MODIS/Terra+Aqua land cover type yearly L3 global 500 m SIN Grid V006. NASA EOSDIS land processes DAAC. From https://doi.org/10.5067/MODIS/MCD12Q1.006. Accessed 11 Mar 2021

Gaughan AE, Stevens FR, Linard C, Jia P, Tatem AJ (2013) High resolution population distribution maps for Southeast Asia in 2010 and 2015. PLoS ONE 8(2):e55882

Georgiou M, Morison G, Smith N, Tieges Z, Chastin S (2021) Mechanisms of impact of blue spaces on human health: a systematic literature review and meta-analysis. Int J Environ Res Public Health 18(5):2486

Giridharan R, Lau SSY, Ganesan S, Givoni B (2008) Lowering the outdoor temperature in high-rise high-density residential developments of coastal Hong Kong: the vegetation influence. Build Environ 43(10):1583–1595

Gunawardena KR, Wells MJ, Kershaw T (2017) Utilising green and bluespace to mitigate urban heat island intensity. Sci Total Environ 584:1040–1055

Hausman JA (1978) Specification tests in econometrics. Econometrica 46:1251–1271

Huang GY (2005) Ecological thinking over spatial structure of hilly city. Urban Plan 29:57–63

Huang Q, Lu Y (2015) The effect of urban heat island on climate warming in the Yangtze River Delta urban agglomeration in China. Int J Environ Res Public Health 12(8):8773–8789

Jin G, Deng X, Zhao X, Guo B, Yang J (2018) Spatiotemporal patterns in urbanization efficiency within the Yangtze River Economic Belt between 2005 and 2014. J Geog Sci 28(8):1113–1126

Levin A, Lin CF, Chu CSJ (2002) Unit root tests in panel data: asymptotic and finite-sample properties. J Econom 108(1):1–24

Li X, Zhou Y, Yu S, Jia G, Li H, Li W (2019) Urban heat island impacts on building energy consumption: a review of approaches and findings. Energy 174:407–419

Luo Q, Luo L, Zhou Q, Song Y (2019) Does China's Yangtze River economic belt policy impact on local ecosystem services? Sci Total Environ 676:231–241

McGarigal K (2015) FRAGSTATS help. University of Massachusetts, Amherst, p 182

Murakawa S, Sekine T, Narita KI, Nishina D (1991) Study of the effects of a river on the thermal environment in an urban area. Energy Build 16(3–4):993–1001

Peng J, Liu Q, Xu Z, Lyu D, Du Y, Qiao R, Wu J (2020) How to effectively mitigate urban heat island effect? A perspective of waterbody patch size threshold. Landsc Urban Plan 202:103873

Peter M (1994) Beyond global warming: ecology and global change beyond global warming: ecology and global change. Ecology 75(7):1861–1876

Pielke RA, Avissar R (1990) Influence of landscape structure on local and regional climate. Landsc Ecol 4(2):133–155

Półrolniczak M, Kolendowicz L, Majkowska A, Czernecki B (2017) The influence of atmospheric circulation on the intensity of urban heat island and urban cold island in Poznań Poland. Theor Appl Climatol 127(3–4):611–625

Pope PT, Webster JT (1972) The use of an F-statistic in stepwise regression procedures. Technometrics 14(2):327–340

Schneider SH (1989) The greenhouse effect: science and policy. Science 243(4892):771–781

Stone B Jr (2005) Urban heat and air pollution: an emerging role for planners in the climate change debate. J Am Plan Assoc 71(1):13–25

Tan X, Sun X, Huang C, Yuan Y, Hou D (2021) Comparison of cooling effect between green space and water body. Sustain Cities Soc 67:102711

Tang LZ, Li ZQ, Yan CF, Sun CH, Xu X, Xiang HR (2009) Mitigative effects of different vegetations on heat island effect in Nanjing. Ecol Environ Sci 18(1):23–28

Unit Root (2021). Retrieved March 26, 2021, from https://en.wikipedia.org/wiki/Unit_root. Retrieved 26 Mar 2021

Xing Z, Wang J, Zhang J (2018) Total-factor ecological efficiency and productivity in Yangtze River Economic Belt, China: a non-parametric distance function approach. J Clean Prod 200:844–857

Yan H, Dong L (2015) The impacts of land cover types on urban outdoor thermal environment: the case of Beijing, China. J Environ Health Sci Eng 13(1):1–7

Yan L, Duarte F, Wang D, Zheng S, Ratti C (2019) Exploring the effect of air pollution on social activity in China using geotagged social media check-in data. Cities 91:116–125

Yang Q, Huang X, Li J (2017) Assessing the relationship between surface urban heat islands and landscape patterns across climatic zones in China. Sci Rep 7(1):1–11

Yu Z, Guo X, Jørgensen G, Vejre H (2017) How can urban green spaces be planned for climate adaptation in subtropical cities? Ecol Ind 82:152–162

Yu Z, Guo X, Zeng Y, Koga M, Vejre H (2018) Variations in land surface temperature and cooling efficiency of green space in rapid urbanization: the case of Fuzhou city, China. Urban for Urban Green 29:113–121

Yu Z, Yang G, Zuo S, Jørgensen G, Koga M, Vejre H (2020) Critical review on the cooling effect of urban blue–green space: a threshold-size perspective. Urban for Urban Green 49:126630

Zeng S, Tian J (2013) Research on microclimatic characteristics of mountainous cities and strategy to mitigate the heat island effect. Archit J S2:106–109

Zhou CH, Cheng WM (2010) Research and compilation of the Geomorphological Atlas of the People's Republic of China. Geogr Res 29(6):970–979